Eur Biophys J (2003) 32: 83–95
DOI 10.1007/s00249-002-0273-8

ARTICLE

A. Ferretti · A. Knijn · C. Raggi · M. Sargiacomo

High-resolution proton NMR measures mobile lipids associated with Triton-resistant membrane domains in haematopoietic K562 cells lacking or expressing caveolin-1

Received: 30 May 2002 / Revised: 6 November 2002 / Accepted: 20 November 2002 / Published online: 28 January 2003

Abstract High-resolution proton NMR spectra of intact tumour cells generally exhibit intense signals due to isotropically mobile lipids (MLs) of still uncertain nature and origin. NMR studies performed on intact wild-type and caveolin-1-infected haematopoietic K562 cells showed that, under our experimental conditions, part of the ML signals are due to lipid complexes resistant to extraction in Triton X-100 at 4 °C. This evidence suggests that a portion of NMR-visible lipid structures are compatible with Triton-resistant membrane rafts and therefore biophysically distinct from NMR-visible Triton-soluble lipid bodies. Similarly to lipid rafts and caveolae, the organization of the Triton-insoluble ML domains could be compromised by treatment with β-octylglucoside or methyl-β-cyclodextrin. Exposure to exogenous sphingomyelinase caused an increase in ML NMR visibility, indicating the possible involvement of ceramides in ML formation. The mobility of these lipids was found to be temperature sensitive, suggesting a transition in cells going from 4 °C to 25–37 °C. These new results are here discussed in the light of possible contributions of plasma membrane microdomains to NMR-visible ML signals.

Keywords Caveolin · Detergent resistance · Membrane microdomains · Mobile lipids · Nuclear magnetic resonance

A. Ferretti and A. Knijn contributed equally to this paper.

A. Ferretti · A. Knijn (✉)
Laboratory of Cell Biology,
Istituto Superiore di Sanità, Viale Regina Elena 299,
00161 Rome, Italy
E-mail: knijn@iss.it
Tel.: +39-06-49902912
Fax: +39-06-49387176

C. Raggi · M. Sargiacomo
Laboratory of Haematology and Oncology,
Istituto Superiore di Sanità, Viale Regina Elena 299,
00161 Rome, Italy

Present address: A. Knijn
Data Management Service, Istituto Superiore di Sanità,
Viale Regina Elena 299, 00161 Rome, Italy

Introduction

Proton high-resolution nuclear magnetic resonance (^{1}H HR-NMR) spectra of some intact tumour cells exhibit intense signals due to the acyl chains of isotropically mobile lipids (MLs), whose biogenesis and nature are still under investigation, because their appearance in the cells derives from different phenomena. Alternative hypotheses propose that MLs originate from membrane microdomains (Mountford and Wright 1988; Ferretti et al. 1999; Le Moyec et al. 2000), from the overproduction of diacylglycerol in the membrane (Glaser et al. 1970) or from loss of membrane asymmetry (Mannechez et al. 2001) and/or from cytoplasmic lipid droplets (Callies et al. 1993; Ferretti et al. 1999; Hakumaki and Kauppinen 2000), which may be formed in the cell under a variety of conditions: mobilization of cholesterol from cell membrane to cytosol (Liu and Anderson 1995), from endoplasmic reticulum and mitochondrial enzyme complexes (Murphy and Vance 1999) or from accumulation of glucosylceramide due to the activation of glucosylceramide synthase (Morjani et al. 2001). Recent studies suggest that plasma membrane microdomains and the membrane surrounding cytoplasmic lipid bodies may represent distinct, but functionally connected, platforms of a more complex network of structures and mechanisms committed to maintain cholesterol homeostasis and subcellular distribution of molecular components involved in cellular signalling (Fujimoto et al. 2001; Ostermeyer et al. 2001; Pol et al. 2001; van Meer 2001).

On the other hand, over the past few years, in studies directed at the structural organization of the plasma membrane, major clues have been offered by the evidence that distinct membrane microdomains (rafts),

with a specific lipid composition (enriched in cholesterol and sphingolipids), can be isolated from mammalian cells. Under biochemical procedures, based upon non-ionic detergent cell extraction (1% Triton X-100 at 4 °C) and sucrose gradient centrifugation, raft domains behave as insoluble membrane fragments with a specific sucrose buoyant density. Because of these unequivocally distinguishable characteristics, we have previously called them low-density Triton-insoluble fractions (LDTI) (Parolini et al. 1996). Most frequently, acronyms like DIG, DRM, GEM (respectively ''detergent-insoluble glycolipid domains'', ''detergent-resistant membranes'' and ''glycolipid-enriched membranes'') are used in the field to indicate the raft's detergent insolubility and glycolipid enrichment. Cholesterol, along with acylated proteins, glycosylphosphatidylinositol (GPI)-anchored proteins and some specific transmembrane proteins, contribute to the raft supramolecular structure. Most importantly, the 22 kDa protein caveolin, when expressed in cells, forms homoligomers, binds cholesterol tightly and is likely to organize rafts in morphologically well-established pit invaginations called caveolae (Sargiacomo et al. 1995; Smart et al. 1999). Since early pioneering studies, a connection between caveolin, cholesterol-sphingolipid plasma membrane domains and a signal function hypothesis has been made (Lisanti et al. 1994). In fact, unusual high levels of well-known signalling proteins such as heterotrimeric G and Src family kinase proteins were found to be concentrated in isolated caveolae (Sargiacomo et al. 1993). Caveolae and rafts are emerging as sites for organizing and sequestering enzymes and their metabolically derived cell signal messengers (ceramides, diglycerides, phosphatidic acid, phosphatidylinositol diphosphate), involved in the regulation of receptor-linked metabolism of sphingomyelin (SM) (Liu and Anderson 1995), phosphatidylcholine (PC) (Czarny et al. 1999; Sciorra and Morris 1999) and phosphoinositides (Stauffer and Meyer 1997). These enzymes, furthermore, form a link between membrane microdomains and rearrangement of the cytoskeleton (Nebl et al. 2000). In addition, a role for the transporter and reversible plasma membrane pool of lipid molecules, like cholesterol, cholesteryl esters and ethers, sphingolipids and free fatty acids, has been recently attributed to rafts and caveolae (Graf et al. 1999; Trigatti et al. 1999; Heino et al. 2000; Vance et al. 2000).

Evidence obtained from haematopoietic cells substantiates the raft-dependent signal transduction hypothesis (Ilangumaran et al. 2000). This is the most complete cell model system to date which implicates rafts in function, including for example the dynamical partitioning of signalling molecules into rafts following T-cell receptor activation (Montixi et al. 1998). By this view, rafts appear as a physiological platform in which molecules directly associate to generate productive signalling cascades.

Recently, a renewed interest of biophysical studies on biomembranes has brought insight into the nature of the physical and chemical forces responsible for the raft lipid organization, causing detergent insolubility at 4 °C (Harder and Simons 1997; Brown and London 1998; Brown 1998). Studies on model membranes demonstrate that phase separation occurs when the differential packing states between glycolipid (tight) and phospholipid (loose) co-exist in distinct ordered phases. The presence of cholesterol in the binary mixture of glycolipids/phospholipids induces the formation of a new physical feature: the ''liquid-ordered phase''. It is characterized by alkyl chains with lateral and rotational diffusion rates comparable to the liquid-crystalline phase, while their freedom of motion is ordered as in the gel phase (Bloom et al. 1991).

Apart from the probable liquid-ordered phase at 4 °C, little is known about the size and dynamics of rafts at physiological temperatures on cell membranes, which are in constant flux due to vesicle traffic, lateral diffusion and metabolic activity. It is still to be determined how to reconcile raft functioning with raft organization. By detecting the existence of non-lamellar lipid pools, and their alterations in intact cells, ^{1}H HR-NMR may in principle provide novel insights on the dynamical lipid structure of membrane domains in their original context, while, most importantly, preserving their original structural organization. We reasoned that if rafts and caveolae are acting as independent constrains of the plasma membrane, they might have a suitably mobile lipid molecular environment, consistent with ^{1}H HR-NMR signal detection in intact cells.

As a first step in the direction of testing this hypothesis, we investigated to what extent Triton-insoluble lipid domains could contribute to the ML signals detected in ^{1}H HR-NMR spectra of the human haematopoietic leukaemia cell line K562. Recently, a speculative hypothesis has been raised to link these K562 ML resonances with no better-specified ''plasma membrane microdomains'' (Le Moyec et al. 2000). Since wild-type K562 cells do not express caveolin-1, we have taken them into account as a system possessing microdomains of the raft type. By analogy, a K562 cell line permanently infected with caveolin-1 has been used as a source of mainly caveolae (Parolini et al. 1999b). These two model systems therefore allowed investigations of the effects exerted on ML signals through modifications induced to rafts and caveolae-like structures. Moreover, by analysis of cell lysates and lipid extracts, a comparison has been made for the cholesterol and phospholipid composition of Triton-insoluble lipid domains in the cells or isolated vesicles (LDTI) observed by NMR. Both procedures of preparation are well established (Moldovan et al. 1995; Parolini et al. 1999a). Finally, the effects were studied of modifications induced on ML signals by (1) changes of temperature from 25 °C to 4 °C and (2) exposure of cells either to exogenous sphingomyelinase or to agents interfering with integral membrane proteins (β-octylglucoside) and cholesterol (methyl-β-cyclodextrin).

Materials and methods

Materials

Methyl-β-cyclodextrin (MCD), sphingomyelinase (SMase from *B. cereus*), cholic acid (sodium salt) and the lipid NMR standards were purchased from Sigma (St. Louis, Mo., USA). 1-*O*-*n*-Octyl-β-D-glucopyranoside (β-octylglucoside, OG) was from Boehringer Mannheim.

Cell culture

Wild-type K562 cells (K562wt) and K562 cells stably infected for the expression of caveolin-1 (K562cav) (40–80×10^6 per sample) were grown in RPMI supplemented with glutamine, antibiotics (penicillin and streptomycin) and 10% fetal bovine serum. Cells were harvested at 72 h (cell density 3–4×10^5/mL).

Expression of caveolin-1 was obtained by a previously described retroviral vector-based gene transfer procedure (Parolini et al. 1999b). Briefly, the caveolin-1 cDNA was inserted into the *Bam*HI site of the wild-type plasmid under the control of the 5' Moloney LTR. This plasmid also separately encodes a form of green fluorescent protein (GFP) under the control of the CMV promoter, allowing transduced cells to be conveniently identified and purified by FACS analysis. The plasmid was transfected by the calcium-phosphate/chloroquine method into the amphotropic packaging cell line Phoenix; viral supernatants were collected after 48 h. For the infection, K562 cells were resuspended at 1×10^5/mL in 0.45 mM filtered viral supernatant, centrifuged for 45 min at 1800 rpm and placed in the incubator for 2 h. Four infection cycles were performed before the cells were placed in growth medium. Infected cells were analysed and sorted following standard procedure by FACS scan (FACS-Vantage; Beckton Dickinson, Omaha, Calif., USA) with a standard excitation wavelength of 488 nm for GFP.

Cells' fixation and detergent treatment

K562wt or K562cav cells (40–80×10^6 per sample) were washed twice in iced PBS. The preparations were subsequently resuspended with 1 mL of 3% paraformaldehyde (PFDH) in PBS, pH 7.2, for 30 min at 4 °C. After washing, samples were either left untreated or treated with 1% Triton X-100 (TX) for 30 min at 4 °C. For comparison, other experiments were performed in which the cells were treated with Triton X-100 without previous PFDH fixation. TX-treated samples were washed three times with PBS to eliminate residual TX. In some experiments the cells were further treated with 60 mM OG in PBS for 30 min at 4 °C, and washed three times with PBS.

Methyl-β-cyclodextrin treatment

Intact K562wt and K562cav cells and also PFDH-fixed and fixed-TX-treated K562wt preparations (60–80×10^6 per sample) were incubated in 2 mL PBS containing 11 mM MCD for 30 min at 37 °C in a rotating thermostatic bath. After these incubations, the samples were centrifuged and the cell pellet was washed with PBS/D_2O at 900×*g* for 5 min before NMR measurements. As a control of the activity of MCD, the first supernatant (kept on ice) of each sample was checked by NMR analyses.

Sphingomyelinase treatment

Intact and fixed-TX-treated K562wt and K562cav cells (60–80×10^6 per sample) were measured by NMR, and subsequently exposed for 35 min at 37 °C to 0.5 U SMase before further NMR analysis. The number of cells did not vary significantly upon treatment.

Total lipid extracts

After the NMR experiments on intact cells the samples were extracted for lipids, following the recommended procedure for the modified method of Svennerholm (Wang and Gustafson 1995). Briefly, cell lysates and treated samples were extracted with 12.5 volumes of methanol added drop by drop, and mixed with a vortex mixer. After 30 min, 6.5 volumes of chloroform were added, and the samples were left for at least 1 h to complete the extraction. The samples were centrifuged for 30 min at 1800×*g* and a second cycle of extraction was applied. The final pooled extract supernatants were evaporated under nitrogen flow. The dried samples were resuspended in either 600 μL $CDCl_3$ plus 300 μL CD_3OD, or in 800 μL $CDCl_3$ only, containing 0.05% TMS for NMR analyses.

Isolation of LDTI from cells

LDTI complexes were isolated as previously described (Lisanti et al. 1994; Parolini et al. 1996). Briefly, 1×10^8 K562 cells were washed and lysed in 1 mL of MBS (25 mM MES, pH 6.5, 150 mM NaCl). Next, both preparations were Dounce homogenized in buffer containing 1% TX and 0.1 mg/mL phenylmethanesulfonyl fluoride, adjusted to 40% sucrose, and placed at the bottom of ultracentrifuge tubes. A 5% to 30% linear sucrose gradient was then placed above the lysate, and the mixture was centrifuged at 45,000 rpm for 16 h at 4 °C in a SW60 rotor (Beckman Instruments, Palo Alto, Calif., USA). In both cases, LDTI complexes, visible as a band migrating at approximately 20% sucrose, were harvested and washed twice with MBS at 14,000 rpm for 30 min at 4 °C. The LDTI fragments were subsequently resuspended in PBS/D_2O before analysis by NMR.

NMR analyses

The ^{31}P NMR analyses of cell lysates were performed following the procedure of Wright et al. (1997), with some modifications. Each cellular sample was dispersed in 0.75 mL isotonic NaCl/D_2O containing 150 mM sodium cholate and 1.0 mM phosphorylcholine, as a standard for signal quantification. NMR spectra (400 scans) of these samples were acquired on a Bruker Avance 400 MHz WB at 161.98 MHz with a 5 mm $^1H/X$ multinuclear inverse probe at 25 °C, applying a 60° pulse (8.3 μs), a pulse delay of 0.8 s and utilizing a sequence with decoupling for protons. For fully relaxed ^{31}P NMR spectra, a 90° pulse was used (12.5 μs) with 20 s of relaxation delay. Assignments were confirmed by measurements on standard samples and by literature (Wright et al. 1997).

The ^1H NMR measurements were performed on either a Varian Gemini 200 MHz (magnetic field 4.7 T), a Bruker Avance 400 MHz WB (9.4 T) or a Bruker AMX 600 MHz (14.1 T) spectrometer at 25 °C to hold metabolic processes under some constraint. Experiments on intact cells were performed by applying a single-pulse (60°) pulse sequence preceded by 1.0 s continuous irradiation for suppression of the water resonance. A spectral width of 12 ppm was measured, corresponding to 2400, 4800 and 7200 Hz at the magnetic fields of 4.7, 9.4 and 14.1 T, respectively. The total measurement time for 320 repetitions was about 17 min, during which cell viability was not compromised. Experiments on total lipid extracts of cells were performed, applying the same pulse sequence as before, this time at the *equilibrium* of magnetization (90° pulses and 5.0 s delay time).

Signal processing and quantitative data analysis of the ^1H NMR spectra of intact and treated cells were performed using the MRUI software package (http://carbon.uab.es/mrui/). Pre-processing of the data consisted in truncation of the final data points to leave the first 2048 points and, if necessary, removal of the residual water signal (at 4.8 ppm), fitting it with 10 exponentials by a Hankel-Lanczos singular value decomposition algorithm; no other pre-processing was applied. The AMARES algorithm (Vanhamme et al. 1997) was used for quantitation directly in the time

(measurement) domain, applying a mathematical model function that consisted of a maximum of 14 Lorentzian components. The number of components depended on the number of resonances present in the spectrum and also included signals not arising from mobile lipids in order to correctly deconvolute the signals of interest. Subsequently, the values for the peak areas were referred to a calibration curve, obtained from measurements on an external standard solution of 50 mM OG in D_2O, and furthermore corrected for the number of cells and (if necessary) the sample volume and the number of repetitions. These measurements were repeated at increasing receiver gain values, in order to compensate for spectrometer non-linearity and variabilities, and were furthermore corrected for the sample volume and the number of cells. With respect to the experiments on intact and treated cells, only quantitative data obtained from the same spectrometer were combined, to avoid the introduction of systematic differences as a function of the applied magnetic field.

Signal processing and quantitative data analysis of the NMR spectra of total lipid extracts were performed using Bruker software, either XWIN-NMR on the spectrometer or WIN-NMR on a personal computer. The 1D spectra were baseline corrected by application of a cubic spline function through appropriate points, after which the peak areas were estimated in the frequency domain by integration. The values for the peak areas were referred to the area of the TMS peak at 0.00 ppm, present in the solvent. Signal assignments were made on the basis of chemical shifts in 1D and cross-correlations in 2D spectra, verified by measurements on standard compounds and literature reports (Adosraku et al. 1994 and references therein).

Results

NMR-visible mobile lipids in intact K562 cells and the effect of the expression of caveolin-1

^{1}H HR-NMR experiments were performed on intact K562wt cells. In agreement with previous reports (Le Moyec et al. 2000), these cells exhibited intense signals arising from ML domains. In the spectrum in Fig. 1A, the characteristic signals of isotropically mobile acyl chains can be recognized, most notably the saturated fraction of the fatty chains [-$(CH_2)_n$-, peak 2 at 1.29 ppm] and terminal methyl groups (-CH_3, peak 1 at 0.89 ppm). Other ML signals arise from α- and β-methylene groups near to a carboxyl group (-O_2C-CH_2-CH_2-, peak 3 at 1.59 ppm, and -O_2C-CH_2-, peak 5 at 2.25 ppm, respectively), methylene groups adjacent to vinyl groups (=CH-CH_2-CH_2-, peak 4 at 2.04 ppm, and =CH-CH_2-CH=, peak 6 at 2.81 ppm) and vinyl groups themselves (=CH-CH=, peak 7 at 5.32 ppm).

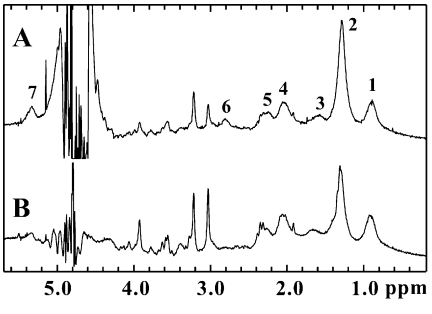

Fig. 1A, B ^{1}H NMR-visible mobile lipid signals in intact K562 cells: effect of formation of caveolae. Spectra measured at 200 MHz on intact packed cells: **A**, K562wt; **B**, K562cav. Main lipid peak assignments: *1*, -CH_3; *2*, -$(CH_2)_n$-; *3*, -O_2C-CH_2-CH_2- + O-CH_2-CH_2- + -CH_2-CH-$(CH_3)_2$; *4*, =CH-CH_2-CH_2- + =CH-CH_2-CH_3; *5*, -O_2C-CH_2-CH_2-; *6*, =CH-CH_2-CH=; *7*, -CH=CH-. The signal at 4.8 ppm is due to not totally suppressed HOD

K562wt cells do not express caveolin-1 and consequently lack caveolae (Parolini et al. 1999b). Infection of K562 cells for the expression of caveolin-1 (K562cav) induces the formation of vesicles, which target for existing rafts where they form caveola structures (Parolini et al. 1999b). ^{1}H HR-NMR measurements were performed on K562cav cells (Fig. 1B) with the scope to ascertain whether the formation of caveolae would affect the NMR visibility of ML domains.

In ^{1}H NMR studies on mobile lipids in intact cells, a parameter *R* has been commonly introduced as the ratio between lipid chain methylene and the terminal methyl protons, i.e. $R = (CH_2)_n/CH_3$. In the literature, only this parameter is usually given in order to avoid complications related to absolute signal quantitation and analysis of minor ML resonances. However, being a relative parameter, *R* is an index of ML NMR visibility, chain length, mobility and/or degree of saturation, rather than simply of ML content, while an increase in ML concentration would cause an increase in both the -$(CH_2)_n$- and -CH_3 signal intensities and could in theory modulate *R* in both directions. In this study, ML signals were quantified in an absolute manner, by applying a mathematical signal-modelling algorithm. The thus-developed method allowed the comparison of measurements between two cell lines in absolute terms as well as in relative terms, and in a more detailed way than that provided by analysing the saturated $(CH_2)_n$ segments only.

Although the spectral pattern appeared to be basically similar for both cell lines, two significant differences occurred (Table 1): the number of lipid acyl chains endowed with isotropic motion decreased in caveolin-1 cells and, furthermore, for the MLs which remained visible, the grade of polyunsaturation per chain decreased. *R* was not significantly different in K562wt and K562cav cells, mostly due to variabilities between different experiments.

Triton-soluble and Triton-insoluble MLs

To investigate the origin of the ML signals present in the spectra of K562wt and K562cav cells, two consecutive treatments were applied to both cell systems: fixation with PFDH followed by incubation with TX at 4 °C, to isolate detergent-resistant membrane domains (TX-treated) and cytoskeleton structures (Moldovan et al. 1995; Parolini et al. 1999a). After fixation with PFDH the cells are dead, but they are still intact. Upon treatment with TX, with regard to the cellular membranes, only TX-resistant structures remain while bulk membrane lipids are extracted (Moldovan et al. 1995). The cytoskeleton is left mainly intact, keeping the cell shape

Table 1 Quantitative changes of ML NMR visibility upon progressive treatments of intact cells[a]

	K562wt	K562cav
Chemical group	Intact ($n=4$)	Intact ($n=3$)
Acyl chains	100%	77 ± 17%*
-($\underline{CH_2}$)$_n$-	9.1 ± 2.2	6.6 ± 0.7
=$\underline{CH}$-$\underline{CH_2}$-CH=	1.2 ± 0.1	0.2 ± 0.3*
=CH-$\underline{CH_2}$-$\underline{CH_2}$-	3.0 ± 0.4	3.2 ± 0.2
R=($\underline{CH_2}$)$_n$/$\underline{CH_3}$	2.17 ± 0.69	1.58 ± 0.28
	PFDH ($n=5$)	PFDH ($n=3$)
Acyl chains	86 ± 34%	82 ± 31%
-($\underline{CH_2}$)$_n$-	10.2 ± 3.6	7.9 ± 4.4
=$\underline{CH}$-$\underline{CH_2}$-CH=	1.0 ± 0.3	0.4 ± 0.5
=CH-$\underline{CH_2}$-$\underline{CH_2}$-	3.2 ± 0.8	2.7 ± 0.8
R=($\underline{CH_2}$)$_n$/$\underline{CH_3}$	2.42 ± 0.61	2.16 ± 0.96
	TX-100 ($n=4$)	TX-100 ($n=2$)
Acyl chains	58 ± 30%	32 ± 1%
-($\underline{CH_2}$)$_n$-	10.8 ± 1.7	11.6 ± 1.7
=$\underline{CH}$-$\underline{CH_2}$-CH=	1.1 ± 0.2	0.8 ± 0.1
=CH-$\underline{CH_2}$-$\underline{CH_2}$-	2.5 ± 0.4	2.8 ± 0.2
R=($\underline{CH_2}$)$_n$/$\underline{CH_3}$	3.33 ± 0.37	3.36 ± 0.56

[a]Quantitative analyses of ML peak areas in the ^{1}H NMR spectra of intact and treated K562 cells (all data measured at 4.7 T). The values for the number of acyl chains are given in arbitrary units (intact, unfixed K562wt = 100% as a reference) and were calculated from the -O_2C-CH_2-CH_2-resonance with respect to β-octylglucoside as external reference; the values for the other ML groups are indicated in number per acyl chain. For comparison with other publications, the parameter R is also given. Significance of the differences between K562wt and K562cav cells was calculated by a two-tailed Student test; differences with P values lower than 0.02 are indicated by an *asterisk*. Abbreviations: *PFDH*, paraformaldehyde-fixed cells; *TX*, cells treated with Triton X-100 after PFDH-fixation; *n*, number of experiments

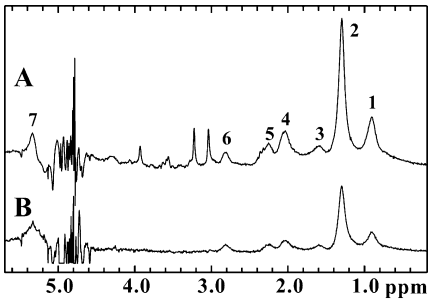

Fig. 2A, B Effect of progressive selective treatments of cells on mobile lipids. ^{1}H NMR spectra measured at 200 MHz on K562wt cells following consecutive treatments: **A**, fixation by paraformaldehyde; **B**, isolation of detergent-resistant domains with Triton X-100 from previously fixed cells. Peak assignments as in Fig. 1

stable; also at the intracellular level, only the TX-insoluble parts remain. The ^{1}H NMR spectra obtained from K562wt cells after fixation and treatment with TX were compared with those of intact cells (examples in Fig. 2, and quantitative results are reported in Table 1).

TX-treated cells preserved a predominant part (at least 50%) of the ML signal intensities for both K562wt and K562cav lines, while the sharp resonances arising from water-soluble metabolites completely disappeared (Fig. 2B). The linewidth of the -(CH_2)$_n$- signal remained similar under all treatments. These results showed for the first time that a relevant part of the ML signals is characterized by Triton insolubility. Contributions to the soluble fraction could arise from: (1) cytoplasmic lipid droplets or other cytoplasmic structures (Rémy et al. 1997; Roman et al. 1997); (2) membrane microdomains, soluble in TX. Lipid droplets seem to be the most likely candidate.

As follows from Table 1, the parameter R was equal (within experimental error) for K562wt and K562cav cells. R increased in TX-treated cells with respect to the intact cells, while the absolute concentration of ML clearly decreased (Table 1), indicating that R mainly reflected variations of mobility.

The observation that a significant part of ^{1}H NMR-visible lipids retained their isotropic mobility, after fixation of the cells, indicates that ML motion does not depend on cell viability. Experiments had demonstrated that fixation with PFDH prior to treatment with TX allowed the detergent to be still effective in isolation of membrane microdomains (Parolini et al 1999b). Furthermore, by fixation, possible modifications of membrane domains upon TX extraction (Harder and Simons 1997) were avoided. PFDH allowed the integrity of the detergent-treated samples to be maintained for a longer period of time and retain their NMR visibility. Besides, it did not alter the ^{1}H NMR spectral pattern, which was of similar intensity to that of TX-treated cells that were analysed without previous PFDH fixation (50% of acyl chains remaining in both unfixed TX-treated and fixed TX-treated cells; data of unfixed cells not shown). The fact that the same values are found for the unfixed TX-treated cells indicated that if some other cellular structure remained after the two consecutive treatments, this was due to their TX insolubility and not to fixation. A parallel experiment has been performed on non-fixed K562wt cells, to study the effect of temperature on TX treatment. With respect to control cells, samples TX-treated at 4 °C retained 54% of the -(CH_2)$_n$- signal, while samples TX-treated at 25 °C retained 4.7% of the -(CH_2)$_n$- signal. Furthermore, samples first TX-treated at 4 °C and then PFDH-fixed and TX-treated at 25 °C retained 11% of the same signal (data not shown).

Plasma membrane origin of MLs

Having established the TX insolubility of a substantial fraction of MLs, experiments were performed to assess whether, and to which extent, membrane ML domains contribute to the total ^{1}H HR-NMR spectrum of intact K562 cells. To this end, the paramagnetic relaxation probe gadolinium (Gd^{3+}) was added to samples of intact cells. Gd^{3+} ions generate a local magnetic field, causing a line broadening to the proton resonances only in close vicinity. Therefore, under the assumption that Gd^{3+} ions do not enter the cells (Mountford et al. 1982), membrane-associated molecules can be distinguished from intracellular molecules. In the experiment, increasing concentrations of $GdCl_3$ were added to a

sample of intact K562wt cells and NMR measurements performed as shown in Fig. 3A–F. Addition of 0.1 mM Gd^{3+} caused 37% of the ML signals to broaden beyond HR visibility, while higher concentrations of the paramagnetic salt further reduced these signals. After the first addition there is a broadening of the choline peak at 3.2 ppm that we cannot explain very well. However, quantifications demonstrated that its intensity remained stable upon the subsequent additions while the ML signals continued to broaden. Furthermore, in parallel experiments performed on intact cells, numerous sharp intracellular signals, for instance lactate, were not broadened after treatment with gadolinium (also here, ML signals were broadened) and did not have their intensity decreased (data not shown). If gadolinium had entered the cells, these should have been broadened at least in part.

Overall, these results indicate that a substantial fraction of MLs reside at the plasma membrane level in these cells. Moreover, for these ML chains to be within the range of action of Gd^{3+}, there are three possibilities: the MLs are (1) located mainly in the outer monolayer; (2) organized in a non-lamellar phase, thus that Gd^{3+} reaches the inner monolayer; (3) in rapid exchange between the inner and outer monolayer.

Analysis of total lipid extracts

Total cellular lipid extracts were analysed by ^{1}H NMR. In this case, all protons give rise to narrow HR-NMR signals whose area only depends upon the concentration of individual proton groups, losing any memory about their original biophysical environment; bilayer lipids become indistinguishable from MLs, and lipids that were first only partly visible, become totally visible.

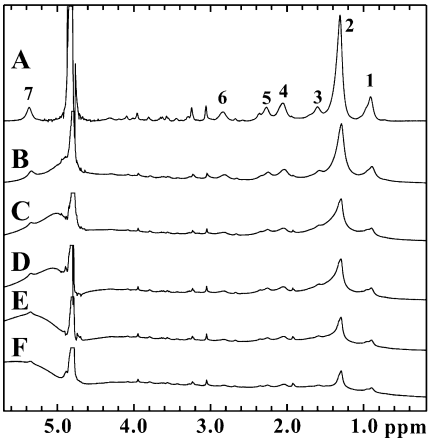

Fig. 3A–F Effect of the addition of gadolinium on mobile lipids. ^{1}H NMR spectra measured at 400 MHz on a sample of intact packed K562wt cells upon addition of increasing concentrations of $GdCl_3$. **A**, before addition; **B–F**, total concentration of added $GdCl_3$: **B**, 0.1 mM; **C**, 0.2 mM; **D**, 0.3 mM; **E**, 0.5 mM; **F**, 1.0 mM. Peak assignments as in Fig. 1

Figure 4 shows the representative spectrum of a total lipid extract of K562wt cells after extraction with TX; peak assignments are reported in the legend. The total $-(CH_2)_n-$ signal arises from phospholipids, glycolipids and neutral lipids present in the sample. This spectrum shows that the concentration of linoleic acid (18:2, peak 22) is very low. The signals from long polyunsaturated fatty acids (20:5, 22:6, peaks 5 and 21) are maintained in the TX-treated cells, consistent with the presence of a significant amount of unsaturated acyl chains, as shown in Table 1. K562 cells are peculiar in that they posses an alternative pathway for uncommon PUFA biosynthesis, involving Δ^5-desaturase and lacking Δ^6-desaturase, which modifies the composition and physical properties of K562 cell membranes (Naval et al. 1993). Spectra of total lipid extracted from K562cav cells were very similar to those of K562wt in possessing signals from polyunsaturated lipids. Comparison with the spectra of the respective intact cells, which showed less intense signals due to polyunsaturated chains, suggests that polyunsaturated lipids may be less mobile rather than less concentrated in intact K562cav cells.

The concentration of cholesterol as calculated from total lipid extracts maintained relatively high levels in the TX-treated cells; in fact, 65% and 57% of the original amount of this compound was preserved, against percentages of 38% and 31% for the other lipids, with respect to PFDH-fixed and intact cells, respectively. Quantification of the C18 methyl resonance of total cholesterol (peak 1) gave a value of 40 ± 9 nmol/10^6 cells in this K562wt cell line and the ratio between cholesterol and PC plus SM (peaks 24 and 25), as measured from the C18 and the $-N^+(CH_3)_3$ signals respectively, was 0.49 ± 0.16 determined in the total lipid extracts of intact cells and increased to 2.6 ± 1.4 in TX-treated cells. The ratio of PC to SM was 5.0 in intact cells and 2.5 in TX-treated cells. These results demonstrated that the detergent-insoluble ML fraction was selectively enriched in SM and in total cholesterol, with respect to the total pool of cellular lipids.

The spectra of either intact or lipid-extracted samples of detergent-treated cells never showed the characteristic signals of TX (at 0.6, 3.5–3.8 and 7.0 ppm), indicating that the detergent was sufficiently removed by washing the cells prior to NMR analyses.

Specific enrichment of MLs in Triton-resistant domains

Figure 5 (upper two parts) shows the percentage of $-(CH_2)_n-$ segments which were NMR visible in either intact K562wt or K562cav cells, as well as in their PFDH-fixed or TX-treated cell preparations. The reported percent values were referred to the total amount of $-(CH_2)_n-$ segments in total lipid extracts of intact K562wt cells. PFDH fixation caused a decrease in the total lipid content, but mainly of lipids that did not possess isotropic mobility. As expected, the subsequent

treatment with TX further reduced the total amount of lipids, while at the same time their relative ML fraction increased for both K562wt and K562cav. The preferential localization of MLs within the TX-insoluble fraction is made more clear by inspection of the lower part of Fig. 5, in which the ratio of NMR-visible ML to the total lipids is shown.

Characterization of TX-insoluble MLs

Given the presence of MLs in the cellular TX-insoluble fraction, in the second part of this study we have focused on the biochemical and biophysical characterization of the NMR-visible structures. To this end, the cells were exposed to specific treatment expected to interfere with the biophysical organization of these structures, as well as with their lipid composition. The results of these experiments are given in Fig. 6A–E.

Temperature dependence of ML signals

Since rafts and caveolae are detergent resistant at 4 °C but not at 25 °C (Melkonian et al. 1995), the possibility

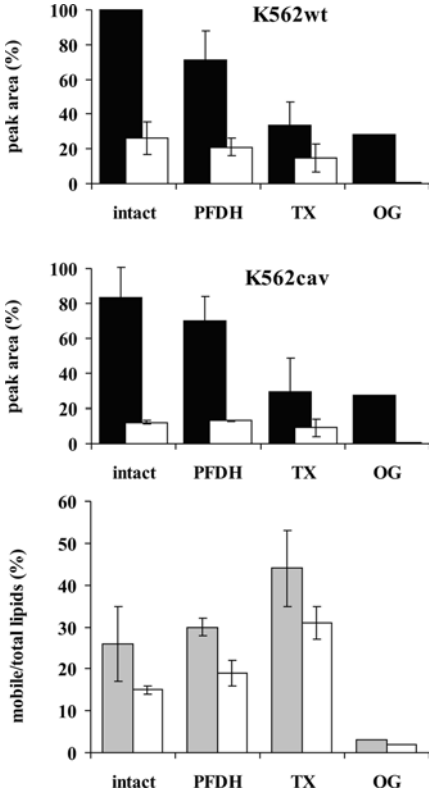

Fig. 5 Quantitative changes of total and mobile lipids upon progressive treatments of cells. Histogram of the -$(CH_2)_n$- groups of (*upper*) K562wt and (*middle*) K562cav cells. Indicated is the quantified NMR peak area, either measured on total lipid solvent extracts (i.e. total lipids, *filled bars*) or on the intact samples (i.e. mobile lipids, *white bars*) under subsequent treatments, relative to their total concentration in the untreated cells (set at 100%) in the same experiment. *Lower*: the relative NMR visibility of the -$(CH_2)_n$- groups (mobile fraction/total concentration) for each specific treatment (K562wt, *filled bars*; K562cav, *white bars*). Abbreviations: *PFDH*, paraformaldehyde-fixed cells; *TX*, cells treated with Triton X-100 after PFDH-fixation; *OG*, β-octylglucoside-treated cells

Fig. 4 Changes in total lipid composition of Triton-resistant membrane domains. ^{1}H NMR spectra measured at 600 MHz on total lipid extracts (in $CDCl_3$ plus CD_3OD) of Triton X-100-treated K562wt cells. *Insert*: a ^{1}H NMR spectrum, measured at 400 MHz and with an enhanced vertical scale, of a total lipid extract of Triton X-100-treated K562wt cells, resuspended in $CDCl_3$ only, to reveal signals in the region around 4.0 ppm which are normally overlapped by the CH_3OD signal. Peak assignments: *1*, cholesterol (C18); *2*, cholesterol (C26 and C27); *3*, -CH_3; *4*, cholesterol (C21); *5*, -CH=CH-CH_2-CH_3; *6*, cholesterol (C19); *7*, cholesterol; *8*, *lyso*-phospholipids?; *9*, -$(CH_2)_n$-; *10*, -CH_2-CH_3; *11*, cholesterol; *12*, -O_2C-CH_2-CH_2-; *13*, -O_2C-CH_2-CH_2-CH_2-CH=CH-; *14*, cholesterol; *15*, cholesterol; *16*, -CH=CH-CH_2-CH_2-; *17*, -O_2C-CH_2-CH_2-CH_2-CH=CH-; *18*, cholesterol; *19*, cholesterol (C4) and sphingolipids; *20*, -O_2C-CH_2-CH_2-; *21*, -O_2C-CH_2-CH_2-CH=CH-; *22*, -CH_2-CH=CH-CH_2-CH=CH-CH_2-; *23*, -CH_2-CH=CH(-CH_2-CH=CH)$_n$-CH_2-; *24*, sphingomyelin [-$^+$N(CH_3)$_3$]; *25*, phosphatidylcholine [-$^+$N(CH_3)$_3$]; *26*, CH_3OD solvent; *27*, cholesterol (C3); *28*, phosphatidylcholine -NH-CH_2-CH_2-O-; *29*, phospholipid and triacylglycerol; *30*, -CH=CH- and cholesterol (C6); *31*, -CH=CH-; *32*, plasmalogens; *33*, phosphatidylinositol (ring); *34*, phospholipids and sphingolipids; *35*, glycerophospholipids and triacylglycerol; *36*, phospholipids, diacylglycerol and triacylglycerol

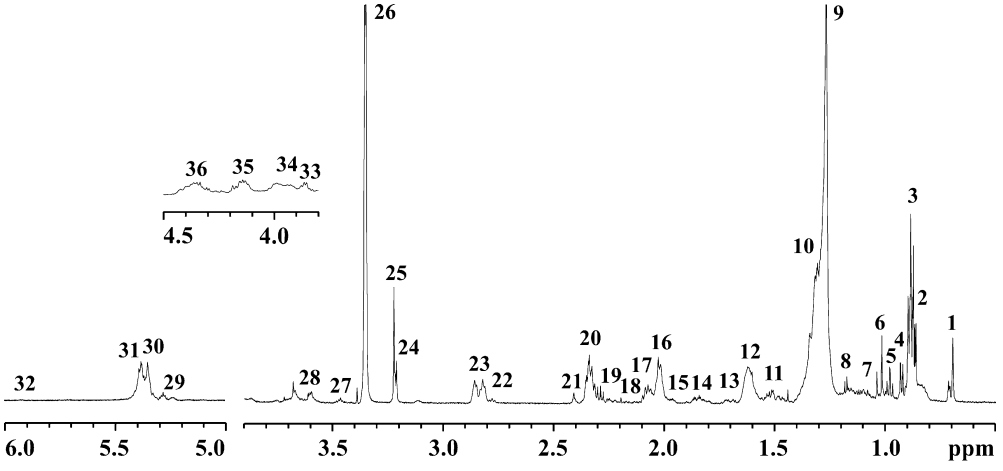

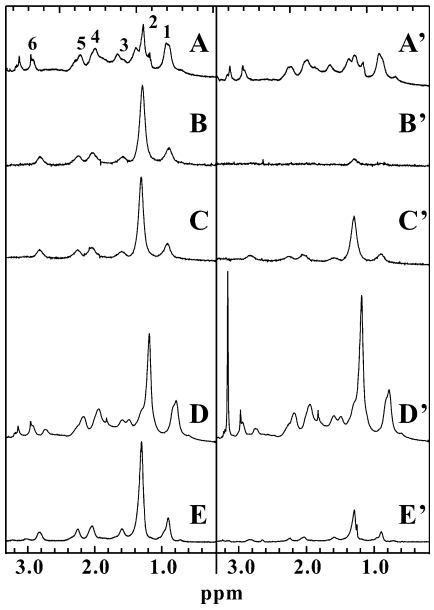

Fig. 6A–E Sensitivity of ML mobility to various treatments. ^{1}H NMR spectra measured on Triton X-100-treated fixed K562wt cells at 25 °C, unless indicated otherwise. **A**, control measured at 25 °C and 400 MHz; **A'**, sample **A** measured at 4 °C; **B**, control at 200 MHz; **B'**, sample from same experiment as **B** treated with 60 mM *β*-octylglucoside; **C**, control at 200 MHz; **C'**, sample **C** treated with 11 mM methyl-*β*-cyclodextrin; **D**, control at 400 MHz; **D'**, sample **D** treated with 0.5 U SMase; **E**, control at 400 MHz; **E'**, sample of LDTI vesicles isolated from K562wt. Peak assignments as in Fig. 1

that ML mobility is affected by temperature was investigated. NMR experiments were performed at both 4 °C and 25 °C on the intact and TX-treated cells, and the results exhibited a substantial decrease in the ML methylene resonance intensity at the lower temperature (Fig. 6A, A'; Table 2). These results are consistent with the hypothesis that detergent-insoluble domains are in a liquid-ordered phase at low temperatures but could change their physical properties at more physiological temperatures.

ML mobility is lost upon treatment with β-octylglucoside

OG is a non-ionic detergent resembling a glycolipid in having a small, polar glucosyl head and long hydrophobic tail. It is thought that the structural similarities between OG and membrane glycolipids allow the detergent to replace the latter in glycolipid-enriched domains, disrupting and/or rearranging lipid/protein organization of rafts and caveolae (Melkonian et al. 1995). OG is described to be a mild detergent that preserves a more native cytoskeleton with respect to TX (Kunimoto et al. 1989). Cell fixation by PFDH does not prevent OG extraction of proteins. While substituting for glycolipids, OG renders GPI-anchored proteins soluble (Melkonian et al. 1995). From Fig. 6B, B' and Table 2, it is clear that OG almost completely disrupted

Table 2 MLs require a specific organization in order to be NMR visible[a]

Cells		OG	MCD	4 °C	SMase	LDTI
Wt	Intact	n.d.	−22%	−49%	+77%	–
	TX[b]	−91%	−46%	−53%	+33%	−80%
Cav	Intact	n.d.	−46%	n.d.	+54%	–
	TX[b]	−93%	n.d.	n.d.	+23%	−80%

[a]The influence of several treatments on the NMR visibility of the ML signals of K562wt and K562cav cells, either intact or TX-treated, was investigated. The variation in intensity of the -$(C\underline{H}_2)_n$- resonance in each treated preparation referenced to its respective control is given. All measurements were performed at 25 °C, with the exception of the measurement at 4 °C. Abbreviations: *TX*, Triton X-100-treated cells; *OG*, *β*-octylglucoside-treated cells; *MCD*, methyl-*β*-cyclodextrin-treated cells; *4* °C, cells measured at 4 °C; *SMase*, sphingomyelinase-exposed cells; *LDTI*, isolated low-density Triton-insoluble vesicles; *n.d.*, not determined

[b]Samples of TX-treated cells with and without prior fixation have been included

ML mobility in both K562wt and K562cav cells, in spite of the fact that most lipids remained present. In fact, after treatment with OG, the quantity of total lipids was substantially unchanged with respect to TX-treated samples, as calculated from the area of the signals still present in the spectra obtained from total lipid extracts of the treated cells. This is in agreement with the reported result that OG does not extract much lipid from rafts and caveolae (Melkonian et al. 1995).

The spectra of washed intact cells did not show OG signals (at 3.2–4.0 and 4.4 ppm) as the molecule has disrupted the mobility of its environment and therefore is NMR invisible itself. In the lipid extracts the OG signals are not revealed, evidently due to the low amount of OG taken up.

NMR visibility of MLs is compromised by removal of plasma membrane cholesterol with methyl-β-cyclodextrin

With its cyclic oligosaccharide structure, MCD forms a hydrophobic cavity, suitable for taking up a cholesterol molecule and shielding it from aqueous solutions, thus greatly enhancing its water solubility. In fact, MCD is efficient and specific in removing cholesterol from the plasma membrane and not toxic under the applied experimental conditions (Kilsdonk et al. 1995). Plasma membrane cholesterol depletion has been described to cause a disruption of raft organization through interruption of the tight association of cholesterol with sphingolipids (Keller and Simons 1998).

In the experiment, intact cells of both K562wt and K562cav lines, and furthermore PFDH- and TX-treated K562wt samples, were measured by ^{1}H HR-NMR, then shortly (30 min) incubated with MCD and re-measured by NMR. For the TX-treated K562wt sample, the spectrum measured before MCD treatment is shown in Fig. 6C and after MCD treatment in Fig. 6C'. As can be appreciated from these spectra, treatment with MCD

resulted in a decrease of ML signals; Table 2 summarizes the quantitative results obtained. MLs in intact K562cav cells were found to be more sensitive to MCD than in intact K562wt. NMR measurements of the first supernatant of each sample showed signals arising from MCD and cholesterol, but not from cell metabolites. No loss of cells was observed. Through quantification of the C18 signal in ^{1}H NMR spectra of total lipid extracts, it was established that, upon MCD treatment, cholesterol was removed by about 50% from intact cells and by 80% from TX-treated cells. As a control, the corresponding amounts of cholesterol were recovered in the ^{1}H NMR spectra of total lipid extracts of the incubation medium.

The result that removal of membrane cholesterol with MCD could reduce the intensity of the ML resonances is another clue that at least part of the MLs is associated with rafts and caveolae. Moreover, in agreement with the effect obtained upon treatment with OG, the result indicates that NMR visibility of MLs depends on lipid organization rather than on their mere presence.

Phospholipid assignments

In order to detect and quantify the phospholipid classes present in TX-treated cells, samples were analysed and characterized by ^{31}P NMR spectroscopy, following the procedure indicated by Wright et al. (1997) based upon the addition of sodium cholate to cell preparations. The quantitative results are given in Table 3.

About 90% of SM was recovered in TX-treated with respect to intact K562wt cells. The PC/SM ratio of 2.6 measured by ^{31}P NMR spectroscopy was in full agreement with that obtained by ^{1}H NMR analysis of lipid extracts.

ML signals are sensitive to sphingomyelinase

NMR is a very suitable technique to monitor the activity of enzymes in the intact cells. Since SMase is described to be present in caveolae and rafts, the effect of exposure of intact and TX-treated fixed cell preparations with this enzyme was followed. In the experiment, the samples were analysed (as a reference), then SMase was exogenously added and the samples were re-measured. Figure 6 shows the spectrum of the same sample of TX-treated K562wt cells before (Fig. 6D) and 35 min after addition of SMase (Fig. 6D'); Table 2 reports the quantitative results. The SM-mediated hydrolysis produced, as expected, an increase in the presence of phosphocholine (signal at 3.2 ppm in Fig. 6D, D'), but also a marked increase in the intensity of the ML signals as measured from their peak area, suggesting that ceramides may be part of the ML domains.

Table 3 Identification and quantification of phospholipids present in the Triton-insoluble fraction[a]

Phospholipid (μmol/10^6 cells)	LDTI	TX	Whole cells
Sphingomyelin	7.25	8.15	8.85
Phosphatidylcholine	22.00	22.54	36.35
Phosphatidylserine	2.30	3.60	5.45
Phosphatidyl-ethanolamine (diacyl + plasmalogen)	6.70	10.48	22.30

[a] ^{31}P NMR analyses of total lipid extracts of K562wt cells. The concentration of the main phospholipids in the TX-treated cells are given in absolute values, calculated with respect to phosphorylcholine as added standard. Abbreviations: *TX*, Triton X-100-treated cells; *LDTI*, isolated low-density Triton-insoluble vesicles

Proton HR-NMR of LDTI vesicles

As the final step of this study, NMR analyses were performed on LDTI vesicles, isolated from K562 cells according to the standard procedures (see Materials and methods), in order to assess whether these structures would also show ML signals. From ESR measurements, LDTI vesicles from RBL-2H3 mast cells were found to be inhomogeneous with part of spin-labelled doubly saturated PCs in the liquid-ordered phase (Ge et al. 1999) and it would be difficult to predict HR-NMR visibility. However, LDTI vesicles, although artefactual to some extent, offer the certainty of measuring exclusively signals arising from raft and caveolae constituents.

A ^{1}H HR-NMR spectrum (400 MHz) of packed LDTI vesicles isolated from K562wt cells is shown in Fig. 6E'. Although low, ML signals could be detected in LDTI, indicating that either the lipid content of these preparations was much lower than that of NMR-visible ML domains in TX-treated cells, or only a small portion of MLs maintained, once isolated, their original isotropic mobility. Since the ^{1}H spectra of LDTI lipid extracts showed a 20-fold increment of the -$(CH_2)_n$- signal with respect to intact LDTI vesicles, and the quantity of total lipids, measured in LDTI extracts, was of the same order as that of the TX preparations, the second interpretation appeared to be correct.

It is also worth noting that, from the LDTI spectrum, it is not possible to resolve HR resonances arising from lipid headgroups. This indicates that the isotropic mobility of NMR-visible lipids in these preparations was not exclusively caused by Brownian motion of the whole LDTI vesicle, nor by lateral diffusion of the lipids around the vesicle. The $N(CH_3)_3$ signals from PC and SM were, however, well visible in the spectra of LDTI lipid extracts and their concentrations determined by ^{31}P NMR (Table 3). Thus, a decisive contribution has to arise from some degree of intrinsic freedom of mobility of the NMR-visible lipid chains up to the α- and β-methylenes. Furthermore, recently, Wright et al. have demonstrated the presence of triacylglycerols in LDTI by thin layer chromatography (L. Wright, personal communication), and the same result has been found for LDTI from K562wt and K562cav cells by thin layer chromatography experiments performed by our group (data not shown).

This finding provides a further clue to the isotropic organization of MLs within the plasma membrane.

LDTI from K562cav cells gave spectra identical to those from K562wt LDTI (data not shown). Overall, their spectral pattern was very similar to that of the TX-treated cells (cf. Fig. 2B) with a parameter $R = 3.4 \pm 1.3$ (8 experiments). However, the areas of the ML signals of the LDTI vesicles were about five times less than that of TX-treated cells, normalized to the quantity of lipids present in total lipid extracts of these samples. This suggests some difference in biophysical and biochemical organization and molecular packing between LDTI, on the one hand, and native rafts and caveolae, on the other.

Discussion

More than 20 years ago, it was first observed that ^{1}H NMR spectra of intact cells can show HR signals (linewidth < 50 Hz) arising from protons of isotropically mobile lipid hydrocarbon chains (Block et al. 1977). Since then, it has been found that different cell lines possess different basic levels of ML signals and, furthermore, that these levels can vary as a function of cell culture conditions. Although modulations in ML signals have been correlated with cell state transitions such as activation, transformation, multidrug resistance, apoptosis and necrosis, still no consensus has been found with respect to the origin of these signals (i.e. nature and localization). Several hypotheses have been postulated for the subcellular location of these NMR-visible lipids making up different structures, residing either at the plasma membrane level [lipoprotein-like structures (Mountford and Wright 1988) or amorphous vesicles (Ferretti et al. 1999)] or in the cytoplasm [lipid bodies/droplets (Barba et al. 1999; Ferretti et al. 1999) or myeloid bodies (Roman et al. 1997)]. It has been demonstrated that lipid bodies are, at least in some cell systems, not the only source of the NMR signals (Ferretti et al. 1999). Therefore, ML signals arise from diverse cellular lipid structures, while relative contributions could vary under different cell states. When performing ^{1}H NMR spectroscopy on intact cells, all protons present in the cells contribute to the spectrum, with either broad-line (linewidth > 500 Hz) or HR signals, dependent on their motion. Proton-bearing chemical groups have to possess rapid as well as isotropic motion in order to give rise to narrow resonances. For instance, the motion of lamellar membrane lipid chain protons, although rapid on the ^{1}H NMR timescale, is anisotropic, because it is restricted to the bilayer plane. Consequently, the signals due to these protons are broad-line and not detectable by ^{1}H HR-NMR techniques (Bloom et al. 1986). The experiments with gadolinium, however, indicate that cellular plasma membranes are able to include domains of isotropically mobile lipids.

In the present study, part of the ML resonances in intact K562 cells have been found to arise from lipids associated with 4 °C TX-insoluble, 25 °C TX-soluble, OG- and MCD-sensitive domains, most likely rafts and caveolae. The responses of ML structures to these various treatments coincide with specific properties of lipid rafts and caveolae. So far, these characteristics have never been described for ML signals. Intracellular lipid bodies have been recently described to posses their own TX-resistant domains (Pol et al. 2001) and could thus possibly contribute to the ML signals. On the other hand, the disappearance of a substantial portion of the ML signals following TX treatment indicates that not all the original visible MLs are retained after solubilization with the detergent. Therefore, the existence of two distinct ML fractions with different biophysical properties has been found. The detergent-labile fraction could be attributed to a population of lipid droplets, in general agreement with Tauchi-Sato et al. (2002).

Caveolae-expressing cells (K562cav) possessed significantly less NMR-visible ML chains and specifically less polyunsaturated ML chains with respect to K562wt cells (see Table 1). These differences disappeared in TX-resistant cell samples, suggesting that in intact cells the expression of caveolin-1 can somehow regulate (in this case negatively) cellular uptake and intracellular trafficking of long-chain fatty acids, as reported by Stremmel et al. (2001), and could enhance the cellular lipid and/or lipoprotein influx/efflux, thus decreasing the cellular ML content (Graf et al. 1999). Furthermore, cells expressing caveolin-1 exhibit in their TX-soluble ML fraction a polyunsaturation grade close to zero. This suggests a role of caveolin-1, possibly in combination with caveolin-2, in cellular lipid metabolism (Ostermeyer et al. 2001) and in the regulation of acyl chain composition of lipids in the two cellular fractions (rafts/caveolae and lipid droplets). Cells expressing caveolae were found to be more sensitive to treatment with MCD than K562wt, which is in total agreement with the notion that caveolin-1, deprived of cholesterol, is severely hindered in its ability to form higher oligomer complexes and caveolar morpho-structures (Li et al. 1996; Kanzaki and Pessin 2002).

Since cholesterol depletion is also effective on raft structures, our experiment with MCD indicates an important parallel between lipid structural organization and ML visibility. On the other hand, OG treatments caused a biophysical lipid change through the removal of integral proteins from the TX-insoluble domains. Lipids, still present as TX-resistant cluster, lose their original NMR-visible organization and implicitly the rapid isotropic motion.

The sensitivity of the ML resonances to the addition of exogenous SMase demonstrated that ceramides can contribute to NMR-visible ML structures and showed the capacity of SMase activity to induce isotropic motion. A hypothesis could be that removal of the typically rigid SM allowed more freedom of movement for the remaining lipids. Apart from the formation of ceramides

in ML structures, this study detected the presence of cholesterol and several phospholipid classes, namely SM, PC, PLA and PS, in the TX-insoluble fraction and in LDTI by means of ^{31}P NMR. Coherent with rafts and caveolae, SM and cholesterol were present in relatively high proportions in TX-treated samples and LDTI. The role of the phospholipids in the organization of ML domains permitting isotropic NMR-visible mobility is still to be ascertained. The evidence, first indicated by the group of Wright (L. Wright, personal communication) and confirmed by our experiments on K562 cells, that LDTI contain neutral lipids provides a clue to the organization of MLs within the plasma membrane. Moreover, this finding may open new aspects on the relation between raft/caveolae and lipid bodies, as well as on how the biological function of caveolins is modulated. While it is unlikely, the results cannot completely discount the possibility that detergent extraction might cause changes in the mobility of existing lamellar lipids. Unlikely also because the responses of the cells to various treatments never changed upon TX treatment. Furthermore, the fraction ML/total lipids increased on going from the intact cell to its TX-treated part and thus the localization of MLs within TX-insoluble domains was found to be specific with respect to the total lipids.

The overall body of evidence implicates important new characteristics for the structural organization of these domains. In fact, the most notable result of this work is the strong evidence that a part of the lipids associated with TX-insoluble membrane rafts and caveolae possesses acyl chains endowed with isotropic mobility. Thus, such mobility well correlates with cellular domains where intense signalling is known to be concentrated.

A peculiarity outlined by this study is the relatively high degree of unsaturation of the ML acyl chains. At first sight, this result seems to contradict what is generally described for the lipid composition of rafts and caveolae. However, tandem mass spectrometric analyses showed 38% of the lipids present in LDTI vesicles from RBL-2H3 mast cells to be polyunsaturated (Fridriksson et al. 1999), most interestingly increasing to more than 50% if the originating cells had previously been stimulated. Furthermore, the lipid anchors of some raft-associated GPI-anchored proteins are characterized by one saturated and one polyunsaturated acyl chain (Schroeder et al. 1998). Thus, contrary to current opinion, polyunsaturated lipids can be abundantly present inside rafts.

Another paradoxical result is the finding of isotropic motion inside domains which are thought to be in the liquid-ordered phase. However, the liquid-ordered phase has not yet been directly demonstrated to exist in cell membranes at physiological temperatures (25–37 °C) (Brown and London 1998). Indeed, the fact that rafts and caveolae are largely TX soluble at these temperatures (Melkonian et al. 1995) indicates some change in their biophysical state with respect to lower temperatures. The NMR analyses performed at 4 °C on intact and TX-treated cells registered a reduction of ML mobility, supporting the hypothesis that at low temperature the structures could be in a liquid-ordered phase, while they change behaviour at physiological temperatures. Furthermore, the measurements on LDTI vesicles suggested a different state between rafts and caveolae either intact on the cell membrane, on the one hand, or isolated as LDTI vesicles, on the other. The lack of the cytoskeleton in LDTI vesicles most surely constitutes a decisive cause for this difference.

From these results, a specialized arrangement of lipids could be hypothesized, located in rafts and caveolae in situ, probably a transition from the lamellar bilayer phase to a non-lamellar phase (Epand 1998; Cullis and De Kruijff 1978). Isotropic non-lamellar phases are known to be promoted by a range of factors under certain circumstances (such as a hydrophobic mismatch between lipid-bilayer thickness and protein transmembrane hydrophobic length, lipid polymorphism, certain peptides, ceramide, phosphatidic acid, diacylglycerol, cholesterol, Ca^{2+}) (Cullis and De Kruijff 1978; Killian et al. 1996 and references therein). Most interestingly, hydrophobic mismatch has also been suggested to be responsible for the formation of membrane lipid domains (Rietveld and Simons 1998). Moreover, according to the same article, caveolae show a morphology at later stages of their development, resembling a bicontinuous cubic membrane. A non-lamellar organization would indicate a possible mechanism for the interaction between the inner and the outer leaflet within rafts. Non-lamellar phases have been implicated in a number of membrane processes, such as exo- and endocytosis, membrane contact and fusion, virus incorporation, transmembrane transport of lipids and proteins, lipid-protein interactions and regulation of enzyme activity (De Kruijff 1987 and references therein; Killian et al. 1996) and in this way could make a link to the involvement of raft and caveolae and their biological roles.

In conclusion, the importance of this study resides in the attribution of the presence of ML signals within TX-insoluble structures in K562 cells and the possibility to explore by NMR in cellular soundness (as in electron microscopy: Moldovan et al. 1995) the mechanisms in which rafts and related domains are involved. Collectively, these results question from which cellular subcompartmentalized structure and/or lipid environment MLs are originated. We have circumscribed to the cholesterol/sphingomyelin/glycolipid-enriched domains a suggestive location where to investigate further.

Acknowledgements At the moment of writing, we discovered that L. Wright et al. (Centre for Infectious Diseases and Microbiology, Westmead Hospital, NSW, Australia) simultaneously and independently have come to the same conclusion, namely that NMR-visible lipid is present in rafts. They have submitted an article describing these results. The authors wish to thank Dr. Franca Podo for reading the manuscript and Massimo Giannini for excellent assistance in assuring top-level performance of MRS equipment.

References

Adosraku RK, Choi GTY, Constantinou-Kokotos V, Anderson MM, Gibbons WA (1994) NMR lipid profiles of cells, tissues, and body fluids: proton NMR analysis of human erythrocyte lipids. J Lipid Res 35:1925–1931

Barba I, Cabañas ME, Arús C (1999) The relationship between nuclear magnetic resonance-visible lipids, lipid droplets, and cell proliferation in cultured C6 cells. Cancer Res 59:1861–1868

Block RE, Maxwell GP, Prudhomme DL, Hudson JL (1977) High resolution proton magnetic resonance spectral characteristics of water, lipid, and protein signals from three mouse cell populations. J Natl Cancer Inst 58:151–156

Bloom M, Holmes KT, Mountford CE, Williams PG (1986) Complete proton magnetic resonance in whole cells. J Magn Reson 69:73–91

Bloom M, Evans E, Mouritsen OG (1991) Physical properties of the fluid lipid-bilayer component of cell membranes: a perspective. Q Rev Biophys 24:293–397

Brown DA, London E (1998) Structure and origin of ordered lipid domains in biological membranes. J Membr Biol 164:103–114

Brown RE (1998) Sphingolipid organization in biomembranes: what physical studies of model membranes reveal. J Cell Sci 111:1–9

Callies R, Sri-Pathmanathan RM, Ferguson DY, Brindle KM (1993) The appearance of neutral lipid signals in the ^{1}H NMR spectra of a myeloma cell line correlates with the induced formation of cytoplasmic lipid droplets. Magn Reson Med 29:546–550

Cullis PR, De Kruijff B (1978) Polymorphic phase behaviour of lipid mixtures as detected by ^{31}P NMR. Evidence that cholesterol may destabilize bilayer structure in membrane systems containing phosphatidylethanolamine. Biochim Biophys Acta 507:207–218

Czarny M, Lavie Y, Fiucci G, Liscovitch M (1999) Localization of phospholipase D in detergent-insoluble, caveolin-rich membrane domains. Modulation by caveolin-1 expression and caveolin-182-101. J Biol Chem 274:2717–2724

De Kruijff B (1987) Polymorphic regulation of membrane lipid composition. Polymorphic regulation of membrane lipid composition. Nature 329:587–588

Epand RM (1998) Lipid polymorphism and protein–lipid interactions. Biochim Biophys Acta 1376:353–368

Ferretti A, Knijn A, Iorio E, Pulciani S, Giambenedetti M, Molinari A, Meschini S, Stringaro A, Calcabrini A, Freitas I, Strom R, Arancia G, Podo F (1999) Biophysical and structural characterization of ^{1}H-NMR-detectable mobile lipid domains in NIH-3T3 fibroblasts. Biochim Biophys Acta 1438:329–348

Fridriksson EK, Shipkova PA, Sheets ED, Holowka D, Baird B, McLafferty FW (1999) Quantitative analysis of phospholipids in functionally important membrane domains from RBL-2H3 mast cells using tandem high-resolution mass spectrometry. Biochemistry 38:8056–8063

Fujimoto T, Kogo H, Ishiguro K, Tauchi K, Nomura R (2001) Caveolin-2 is targeted to lipid droplets, a new "membrane domain" in the cell. J Cell Biol 152:1079–1085

Ge M, Field KA, Aneja R, Holowka D, Baird B, Freed JH (1999) Electron spin resonance characterization of liquid ordered phase of detergent-resistant membranes from RBL-2H3 cells. Biophys J 77:925–933

Glaser M, Simpkins H, Singer SJ, Sheetz M, Chan SI (1970) On the interactions of lipids and proteins in the red blood cell membrane. Proc Natl Acad Sci USA 65:721–728

Graf GA, Connell PM, van der Westhuyzen DR, Smart EJ (1999) The class B, type I scavenger receptor promotes the selective uptake of high density lipoprotein cholesterol ethers into caveolae. J Biol Chem 274:12043–12048

Hakumaki JM, Kauppinen RA (2000) ^{1}H NMR visible lipids in the life and death of cells. Trends Biochem Sci 25:357–362

Harder T, Simons K (1997) Caveolae, DIGs, and the dynamics of sphingolipid-cholesterol microdomains. Curr Opin Cell Biol 9:534–542

Heino S, Lusa S, Somerharju P, Ehnholm C, Olkkonen VM, Ikonen E (2000) Dissecting the role of the golgi complex and lipid rafts in biosynthetic transport of cholesterol to the cell surface. Proc Natl Acad Sci USA 97:8375–8380

Ilangumaran S, He H-T, Hoessli DC (2000) Microdomains in lymphocyte signalling: beyond GPI-anchored proteins. Immunol Today 21:2–7

Kanzaki M, Pessin JE (2002) Caveolin-associated filamentous actin (Cav-actin) defines a novel F-actin struture in adipocytes. J Biol Chem 277:25867–25869

Keller P, Simons K (1998) Cholesterol is required for surface transport of influenza virus hemagglutinin. J Cell Biol 140:1357–1367

Killian JA, Salemink I, de Planque MR, Lindblom G, Koeppe RE II, Greathouse DV (1996) Induction of nonbilayer structures in diacylphosphatidylcholine model membranes by transmembrane alpha-helical peptides: importance of hydrophobic mismatch and proposed role of tryptophans. Biochemistry 35:1037–1045

Kilsdonk EPC, Yancey PG, Stoudt GW, Bangerter FW, Johnson WJ, Phillips MC, Rothblat GH (1995) Cellular cholesterol efflux mediated by cyclodextrins. J Biol Chem 270:17250–17256

Kunimoto M, Shibata K, Miura T (1989) Comparison of the cytoskeleton fractions of rat red blood cells prepared with nonionic detergents. J Biochem (Tokyo) 105:190–195

Le Moyec L, Legrand O, Larue V, Kawakami M, Marie JP, Calvo F, Hantz E, Taillandier E (2000) Magnetic resonance spectroscopy of cellular lipid extracts from sensitive, resistant and reverting K562 cells and flow cytometry for investigating the P-glycoprotein function in resistance reversion. NMR Biomed 13:92–101

Li S, Song KS, Lisanti MP (1996) Expression and characterization of recombinant caveolin. J Biol Chem 271:568–573

Lisanti MP, Scherer PE, Tang Z, Sargiacomo M (1994) Caveolae, caveolin and caveolin-rich membrane domains: a signalling hypothesis. Trends Cell Biol 4:231–235

Liu P, Anderson RGW (1995) Compartmentalized production of ceramide at the cell surface. J Biol Chem 270:27179–27185

Mannechez A, Collet B, Payen L, Lecureur V, Fardel O, Le Moyec L, De Certaines J-D, Leray G (2001) Differentiation of the P-gp and MRP1 multidrug resistance systems by mobile lipid ^{1}H-NMR spectroscopy and phosphatidyl serine externalization. Anticancer Res 21:3915–3920

Melkonian A, Chu T, Tortorella LB, Brown DA (1995) Characterization of proteins in detergent-resistant membrane complexes from Madin-Darby canine kidney epithelial cells. Biochemistry 34:16161–16170

Moldovan NI, Heltianu C, Simionescu N, Simionescu M (1995) Ultrastructural evidence of differential solubility in Triton X-100 of endothelial vesicles and plasma membrane. Exp Cell Res 219:309–313

Montixi C, Langlet C, Bernard AM, Thimonier J, Dubois C, Wurbel MA, Chauvin JP, Pierres M, He HT (1998) Engagement of T cell receptor triggers its recruitment to low-density detergent-insoluble membrane domains. EMBO J 17:5334–5348

Morjani H, Aouali N, Belhoussine R, Veldman RJ, Levade T, Manfait M (2001) Elevation of glucosylceramide in multidrug-resistant cancer cells and accumulation in cytoplasmic droplets. Int J Cancer 94:157–165

Mountford CE, Wright LC (1988) Characterization of transformed cells and tumors by proton nuclear magnetic resonance spectroscopy. Trends Biochem Sci 13:172–177

Mountford CE, Grossman G, Reid G, Fox RM (1982) Organization of lipids in the plasma membranes of malignant and stimulated cells: a new model. Cancer Res 42:2270–2276

Murphy DJ, Vance J (1999) Mechanisms of lipid-body formation. Trends Biochem Sci 24:109–115

Naval J, Martinez-Lorenzo MJ, Marzo I, Desportes P, Pineiro A (1993) Alternative route for the biosynthesis of polyunsaturated fatty acids in K562 cells. Biochem J 291:841–845

Nebl T, Oh SW, Luna EJ (2000) Membrane cytoskeleton: PIP(2) pulls the strings. Curr Biol 10:351–354

Ostermeyer AG, Paci JM, Zeng Y, Lublin DM, Munro S, Brown DA (2001) Accumulation of caveolin in the endoplasmic reticulum redirects the protein to lipid storage droplets. J Cell Biol 152:1071–1078

Parolini I, Sargiacomo M, Lisanti MP, Peschle C (1996) Signal transduction and glycophosphatidylinositol-linked proteins (lyn, lck, CD4, CD45, G proteins, and CD55) selectively localize in Triton-insoluble plasma membrane domains of human leukaemic cell lines and normal granulocytes. Blood 87:3783–3794

Parolini I, Topa S, Sorice M, Pace A, Ceddia P, Montesoro E, Pavan A, Lisanti MP, Peschle C, Sargiacomo M (1999a) Phorbol ester-induced disruption of the CD4-Lck complex occurs within a detergent-resistant microdomain of the plasma membrane. Involvement of the translocation of activated protein kinase C isoforms. J Biol Chem 274:14176–14187

Parolini I, Sargiacomo M, Galbiati F, Rizzo G, Grignani F, Engelman JA, Okamoto T, Ikezu T, Scherer PE, Mora R, Rodriguez-Boulan E, Peschle C, Lisanti MP (1999b) Expression of caveolin-1 is required for the transport of caveolin-2 to the plasma membrane. Retention of caveolin-2 at the level of the golgi complex. J Biol Chem 274:25718–25725

Pol A, Luetterforst R, Lindsay M, Heino S, Ikonen E, Parton RG (2001) A caveolin dominant negative mutant associates with lipid bodies and induces intracellular cholesterol imbalance. J Cell Biol 152:1057–1070

Rémy C, Fouilhé N, Barba I, Sam-La E, Lahrech H, Cucurella M-G, Izquierdo M, Moreno A, Ziegler A, Massarelli R, Décorps M, Arús C (1997) Evidence that mobile lipids detected in rat brain glioma by ^{1}H nuclear magnetic resonance correspond to lipid droplets. Cancer Res 57:407–414

Rietveld A, Simons K (1998) The differential miscibility of lipids as the basis for the formation of functional membrane rafts. Biochim Biophys Acta 1376:467–479

Roman SK, Jeitner TM, Hancock R, Cooper WA, Rideout DC, Delikatny EJ (1997) Induction of magnetic resonance-visible lipid in a transformed human breast cell line by tetraphenylphosphonium chloride. Int J Cancer 73:570–579

Sargiacomo M, Sudol M, Tang ZL, Lisanti MP (1993) Oligomeric structure of caveolin: implications for caveolae membrane organization. J Cell Biol 122:789–807

Sargiacomo M, Scherer PE, Tang Z, Kubler E, Song KS, Sanders MC, Lisanti MP (1995) Signal transducing molecules and glycosyl-phosphatidylinositol-linked proteins form a caveolin-rich insoluble complex in MDCK cells. Proc Natl Acad Sci USA 92:9407–9411

Schroeder RJ, Ahmed SN, Zhu Y, Condor E, Brown DA (1998) Cholesterol and sphingolipid enhance the Triton X-100 insolubility of glycosylphosphatidylinositol-anchored proteins by promoting the formation of detergent-insoluble ordered membrane domains. J Biol Chem 273:1150–1157

Sciorra VA, Morris AJ (1999) Sequential actions of phospholipase D and phosphatidic acid phosphohydrolase 2b generate diglyceride in mammalian cells. Mol Biol Cell 10:3863–3876

Smart EJ, Graf GA, McNiven MA, Sessa WC, Engelman JA, Scherer PE, Okamoto T, Lisanti MP (1999) Caveolins, liquid-ordered domains, and signal transduction. Mol Cell Biol 19:7289–7304

Stauffer TP, Meyer T (1997) Compartmentalized IgE receptor-mediated signal transduction in living cells. J Cell Biol 139:1447–1454

Stremmel W, Pohl L, Ring A, Herrmann T (2001) A new concept of cellular uptake and intracellular trafficking of long-chain fatty acids. Lipids 36:981–989

Tauchi-Sato K, Ozeki S, Houjou T, Taguchi T, Fujimoto T (2002) The surface of lipid droplets is a phospholipid monolayer with a unique fatty acid composition. J Biol Chem, published on-line as manuscript M207712200

Trigatti BL, Anderson RGW, Gerber GE (1999) Identification of caveolin-1 as a fatty acid binding protein. Biochem Biophys Res Commun 255:34–39

Vance JE, Campenot RB, Vance DE (2000) The synthesis and transport of lipids for axonal growth and nerve regeneration. Biochim Biophys Acta 1486:84–96

Vanhamme L, van den Boogaart A, van Huffel S (1997) Improved method for accurate and efficient quantification of MRS data with use of prior knowledge. J Magn Reson 129:35–43

Van Meer G (2001) Caveolin, cholesterol, and lipid droplets? J Cell Biol 152:F29–F34

Wang W-Q, Gustafson A (1995) Ganglioside extraction from erythrocytes: a comparison study. Acta Chem Scand 49:929–936

Wright LC, Nouri-Sorkhabi MH, May GL, Danckwerts LS, Kuchel PW, Sorrel TC (1997) Changes in cellular and plasma membrane phospholipid composition after lipopolysaccharide stimulation of human neutrophils, studied by ^{31}P NMR. Eur J Biochem 243:328–335